

See discussions, stats, and author profiles for this publication at: <https://www.researchgate.net/publication/7600493>

High-order discretization schemes for biochemical applications of boundary element solvation and variational electrostatic projection methods

ARTICLE *in* THE JOURNAL OF CHEMICAL PHYSICS · JUNE 2005

Impact Factor: 2.95 · DOI: 10.1063/1.1899146 · Source: PubMed

CITATIONS

7

READS

29

2 AUTHORS, INCLUDING:



[Brent A Gregersen](#)

D. E. Shaw Research

19 PUBLICATIONS 838 CITATIONS

SEE PROFILE

High-order discretization schemes for biochemical applications of boundary element solvation and variational electrostatic projection methods

Brent A. Gregersen and Darrin M. York^{a)}

Department of Chemistry, University of Minnesota, 207 Pleasant St. SE, Minneapolis, MN 55455, USA.

Received Date: February 9, 2005.

A series of high-order surface element discretization schemes for variational boundary element methods are introduced. The surface elements are chosen in accord with angular quadrature rules for integration of spherical harmonics. Surface element interactions are modeled by Coulomb integrals between spherical Gaussian functions with exponents chosen to reproduce the exact variational energy and Gauss' law for a point charge in a spherical cavity. The present work allows high-order surface element expansions to be made for variational methods such as the conductor-like screening model for solvation and the variational electrostatic projection method for generalized solvent boundary potentials in molecular simulations.

Two methods that have an important role in the arsenal of "multi-scale" modeling techniques used to calculate reactions of biomolecules are the smooth conductor-like screening model (COSMO)¹ and the recently introduced variational electrostatic projection (VEP) method.² The smooth COSMO model is based on a conductor variational principle originally proposed by Klamt and Schüürmann,³ but differs from their original method in that the surface elements are modeled by Gaussian functions that can be smoothly switched off or on as they become buried or exposed with changes in molecular geometry. The smooth COSMO method has recently been extended to electronic structure and hybrid QM/MM methods⁴ and applied to phosphoryl transfer reactions in solution.⁵ The VEP method² has been used to model the macromolecular electrostatic environment in stochastic boundary molecular dynamics simulations.

The smooth COSMO and VEP methods are variational *boundary element* techniques that use discretized Gaussian surface elements that require specification of surface element position *and* properly calibrated Gaussian exponents to provide the correct variational response. In the present work, a prescription for determination of the discretized surface elements and their Gaussian exponents is derived based on numerical quadrature rules for integration of spherical harmonics. The data and relations presented here provide a convenient mechanism whereby boundary element methods such as smooth COSMO and VEP can be extended to very high order.

Angular quadrature rules

The surface discretization procedures used in the present work are based on angular quadrature rules⁶ for spherical harmonic functions.⁷ These rules are ideally suited for the smooth COSMO and VEP methods that may use constraints on high-order multipole moments in the variational procedure.

^{a)}Electronic mail: york@chem.umn.edu

The set of N angular quadrature points $\{\theta_i, \phi_i\}$ and weights $\{w_i\}$ (normalized to 4π), for $i = 1, \dots, N$, for a particular order are determined to satisfy the integral relation

$$\int_0^{2\pi} d\phi \int_{-1}^1 d(\cos \theta) f(\theta, \phi) = \sum_{i=1}^N w_i f(\theta_i, \phi_i) \quad (1)$$

where the function $f(\theta, \phi)$ can be represented in a basis of spherical harmonic functions up to a fixed order L as

$$f(\theta, \phi) = \sum_{l=0}^L \sum_{m=-l}^l C_{l,m} Y_{l,m}(\theta, \phi) \quad (2)$$

where $Y_{l,m}(\theta, \phi)$ is a spherical harmonic function and $C_{l,m}$ is the corresponding expansion coefficient.

Two types of angular quadrature rules⁶ are considered: 1) a Gauss-Legendre product, and 2) Lebedev grid. The Gauss-Legendre product formula requires $L + 1$ equally spaced points and uniform weights in ϕ , and $(L + 1)/2$ Gauss-Legendre⁸ quadrature points and weights in $\cos \theta$. This leads to a set of $N_{GL} = (L + 1)^2/2$ angular quadrature points that gives exact integration up to order L on the unit sphere. A more efficient set of angular quadrature for spherical harmonic functions, first pioneered by Lebedev,^{9,10} involves formulas for specific points and weights determined algebraically. These angular quadrature grids were later extended^{11,12} and recently to very high order by Laikov.¹³ For the Lebedev grid methods, the number of quadrature points required to satisfy exact integral relations up to order L is approximately $N_{Leb} \approx (L + 1)^2/3$, resulting in a computational cost reduction of about 33% relative to Gauss-Legendre.

Discretized surface elements

The discretized surfaces (henceforth be designated by γ) used in the smooth COSMO¹ and VEP² methods are based on discretized unit spheres that can then be dilated using exact scaling relations, translated and assembled. The surface elements are represented by smooth Gaussian functions of the form

$$g_i(\mathbf{r}) = \left(\frac{\zeta_i^2}{\pi}\right)^{3/2} e^{-\zeta_i^2 |\mathbf{r} - \mathbf{r}_i|^2} \quad (3)$$

where \mathbf{r}_i is the position of the i th surface element and ζ_i is the Gaussian exponent. The electrostatic interaction between surface elements i and j are modeled by the Coulomb integrals

$$J_{ij} = \int \int \frac{g_i(\mathbf{r}) g_j(\mathbf{r}')}{|\mathbf{r} - \mathbf{r}'|} d^3r d^3r' = \frac{\text{erf}(\zeta_{ij} r_{ij})}{r_{ij}} \quad (4)$$

where $\zeta_{ij} = \zeta_i \zeta_j / \sqrt{\zeta_i^2 + \zeta_j^2}$, $r_{ij} = |\mathbf{r}_i - \mathbf{r}_j|$, and $\text{erf}(x)$ is the error function.⁷ The surface element self interaction is determined in the limit that $\zeta_i = \zeta_j$ and $r_{ij} \rightarrow 0$, and is given by

$$J_{ii} = \int \int \frac{g_i(\mathbf{r}) g_i(\mathbf{r}')}{|\mathbf{r} - \mathbf{r}'|} d^3r d^3r' = \sqrt{\frac{2}{\pi}} \zeta_i \quad (5)$$

and the interaction of the Gaussian surface elements at \mathbf{r}_i with a unit point charge at \mathbf{R}_j can be calculated from Eq. 4 in the limit that $\zeta_j \rightarrow \infty$ to give

$$B_{ij} = \int \int \frac{g_i(\mathbf{r})\delta(\mathbf{r}' - \mathbf{R}_j)}{|\mathbf{r} - \mathbf{r}'|} d^3r d^3r' = \frac{\text{erf}(\zeta_i|\mathbf{r}_i - \mathbf{R}_j|)}{|\mathbf{r}_i - \mathbf{R}_j|} \quad (6)$$

The matrix elements of Eqs. 4, 5 and 6 correspond to the matrix elements of Eqs. 66, 67 and 72, respectively, in the smooth COSMO method,¹ and Eqs. 9, 12 and 13, respectively, in the VEP method.²

These Gaussian exponents, ζ_i , satisfy a simple relation with the angular quadrature weights w_i on the unit sphere:

$$\zeta_i = \zeta / \sqrt{w_i} \quad (7)$$

where ζ is a scale factor chosen for each quadrature rule to reproduce the variational energy and Gauss' law surface charge for a point charge Q at the center of a unit sphere (Eq. 7 is appropriate for rules where $w_i > 0 \forall i$). The relation between the surface element and the Gaussian exponent (Eq. 7) results in a nearly uniform variational surface charge distribution γ_i

$$\gamma_i = Qw_i/4\pi \quad (8)$$

For spheres of different radii R , the discretization points, weights and Gaussian exponents obey the exact scaling relations

$$\zeta_i(R) = \zeta_i/R = \zeta/\sqrt{w_i(R)} \quad (9)$$

$$\mathbf{r}_i(R) = \mathbf{r}_i \cdot R \quad (10)$$

$$w_i(R) = w_i \cdot R^2 \quad (11)$$

where \mathbf{r}_i , w_i and ζ_i correspond to the discretized unit sphere. The purpose of the present work is to present the scale factors ζ for a wide range of high-order quadrature rules such that they can be used to generate systematic sets of discretized γ surfaces for smooth COSMO, VEP and other boundary-element methods.

Scale factors for Gaussian exponents

Tables I and II list the optimized values of the scale factors, ζ of Eq. 7, for each discretization level, along with the root-mean-square (rms) error ($\sigma_\gamma = \langle (\gamma^{calc} - \gamma)^2 \rangle^{1/2}$) in the variational γ surface charge distribution (Eq. 8), and the relative rms error ($\sigma_\gamma^{rel} = \sigma_\gamma / \langle \gamma^2 \rangle^{1/2}$). All of the surface element discretization schemes beyond 8 points give numerical values for the variational energy and Gauss' law surface charge to at least 12 significant figures. The surface elements derived from all of the quadrature rules produce nearly uniform variational surface charge distributions. The σ_γ values for the Gauss-Legendre surface elements fall below 10^{-4} with 242 points (order 21) or greater and fall below 10^{-5} with 1058 points (order 45) or greater, reaching the lowest σ_γ value of 10^{-6} at 5000 points (order 99). The Lebedev grids converge more quickly in terms of

integration order and require less discretization points than the Gauss-Legendre product rules. The σ_γ values for the Lebedev surface elements fall below 10^{-4} , 10^{-5} , and 10^{-6} with 50, 434, and 1202 points, respectively, corresponding to orders 11, 35 and 59, respectively. The lowest σ_γ value of 4.6×10^{-8} occurs at 5810 points (order 131).

The scale factors, ζ , can be fit to the number of surface elements N_γ with the empirical equation

$$\zeta = c_0 + c_1/(N_\gamma + c_2)^{1/n} \quad (12)$$

where c_0 , c_1 and c_2 are unitless empirical parameters and n is an integer. Plots of the Gaussian exponent scale factors for the Gauss-Legendre and Lebedev surface elements as a function of $N_\gamma^{1/2}$ are shown in Fig. I. Although the fit to Eq. 12 is very good, it is recommended that the scale factors from Tables I and II be used for quantitative work.

The present work offers a prescription for the generation of discretized surface elements for variational boundary element methods such as smooth COSMO and VEP that are important for modeling reactions of biomolecules with multi-scale models. Extension to high order discretization allows the accuracy of the methods to be systematically improved, the convergence properties to be characterized and benchmark quality calculations to be performed.

Acknowledgment. The authors thank Dr. Dimitri Laikov for constructive comments on the angular quadrature methods. DY is grateful for financial support provided by the National Institutes of Health (grant GM62248) and the Army High Performance Computing Research Center (AHPCRC) under the auspices of the Department of the Army, Army Research Laboratory (ARL) under Cooperative Agreement number DAAD19-01-2-0014. Computational resources were provided by the Minnesota Supercomputing Institute.

References

- ¹ D. M. York and M. Karplus, *J. Phys. Chem. A* **103**, 11060 (1999).
- ² B. A. Gregersen and D. M. York, *J. Phys. Chem. B* **109**, 536 (2005).
- ³ A. Klamt and G. Schüürmann, *J. Chem. Soc. Perkin Trans. 2* **2**, 799 (1993).
- ⁴ J. Khandogin, B. A. Gregersen, W. Thiel, and D. M. York. *J. Phys. Chem. B*, *in press*.
- ⁵ B. A. Gregersen, J. Khandogin, W. Thiel, and D. M. York. *J. Phys. Chem. B*, *in press*.
- ⁶ A. H. Stroud, *Approximate Calculation of Multiple Integrals* (Prentice Hall, Englewood Cliffs, 1971).
- ⁷ G. B. Arfken and H. J. Weber, *Mathematical methods for physicists*, 5 ed. (Academic Press, San Diego, 2001).
- ⁸ W. H. Press, S. A. Teukolsky, W. T. Vetterling, and W. P. Flannery, *Numerical Recipes in Fortran*, 2 ed. (Cambridge University Press, Cambridge, 1992).
- ⁹ V. I. Lebedev, *Ž. Vyčisl. Mat. i Mat. Fiz.* **15**, 48 (1975).
- ¹⁰ V. I. Lebedev, *Ž. Vyčisl. Mat. i Mat. Fiz.* **16**, 293 (1976).
- ¹¹ V. I. Lebedev, *Russ. Acad. Sci. Dokl. Math.* **50**, 283 (1995).
- ¹² B. Delley, *J. Comput. Chem.* **17**, 1152 (1996).
- ¹³ V. I. Lebedev and D. N. Laikov, *Russ. Acad. Sci. Dokl. Math.* **59**, 477 (1999). Angular quadrature parameters available from <http://server.ccl.net/cca/software/SOURCES/FORTRAN/Lebedev-Laikov-Grids/index.shtml>.

TABLE I: Optimized scale factor for Gaussian exponents for Gauss-Legendre product quadrature rules.

| N_γ | Order | ζ | σ_γ^{rel} | σ_γ |
|------------|-------|---------------|-----------------------|-----------------|
| 8 | 3 | 4.81422286657 | 5.6E-08 | 7.0E-09 |
| 18 | 5 | 4.80355317623 | 1.4E-02 | 7.8E-04 |
| 32 | 7 | 4.78929182220 | 2.2E-02 | 7.3E-04 |
| 50 | 9 | 4.78046194039 | 2.6E-02 | 5.4E-04 |
| 72 | 11 | 4.77441939471 | 2.6E-02 | 3.8E-04 |
| 98 | 13 | 4.76987757037 | 2.4E-02 | 2.7E-04 |
| 128 | 15 | 4.76627339659 | 2.3E-02 | 1.9E-04 |
| 162 | 17 | 4.76331034085 | 2.1E-02 | 1.4E-04 |
| 200 | 19 | 4.76081164022 | 2.0E-02 | 1.1E-04 |
| 242 | 21 | 4.75866434329 | 1.8E-02 | 8.1E-05 |
| 288 | 23 | 4.75679242121 | 1.7E-02 | 6.4E-05 |
| 338 | 25 | 4.75514229420 | 1.6E-02 | 5.1E-05 |
| 392 | 27 | 4.75367465448 | 1.5E-02 | 4.1E-05 |
| 450 | 29 | 4.75235967933 | 1.4E-02 | 3.4E-05 |
| 512 | 31 | 4.75117411875 | 1.3E-02 | 2.8E-05 |
| 578 | 33 | 4.75009944840 | 1.3E-02 | 2.4E-05 |
| 648 | 35 | 4.74912064899 | 1.2E-02 | 2.0E-05 |
| 722 | 37 | 4.74822536875 | 1.1E-02 | 1.7E-05 |
| 800 | 39 | 4.74740332938 | 1.1E-02 | 1.5E-05 |
| 882 | 41 | 4.74664589270 | 1.0E-02 | 1.3E-05 |
| 968 | 43 | 4.74594573694 | 9.9E-03 | 1.1E-05 |
| 1058 | 45 | 4.74529661002 | 9.6E-03 | 9.9E-06 |
| 1152 | 47 | 4.74469313824 | 9.2E-03 | 8.8E-06 |
| 1250 | 49 | 4.74413067576 | 8.9E-03 | 7.8E-06 |
| 1352 | 51 | 4.74360518477 | 8.5E-03 | 7.0E-06 |
| 1458 | 53 | 4.74311313892 | 8.3E-03 | 6.2E-06 |
| 1568 | 55 | 4.74265144483 | 8.0E-03 | 5.6E-06 |
| 1682 | 57 | 4.74221737774 | 7.7E-03 | 5.1E-06 |
| 1800 | 59 | 4.74180852838 | 7.5E-03 | 4.6E-06 |
| 1922 | 61 | 4.74142275878 | 7.3E-03 | 4.2E-06 |
| 2048 | 63 | 4.74105816525 | 7.1E-03 | 3.8E-06 |
| 2178 | 65 | 4.74071304736 | 6.9E-03 | 3.5E-06 |
| 2312 | 67 | 4.74038588161 | 6.7E-03 | 3.2E-06 |
| 2450 | 69 | 4.74007529910 | 6.5E-03 | 2.9E-06 |
| 2592 | 71 | 4.73978006650 | 6.3E-03 | 2.7E-06 |
| 2738 | 73 | 4.73949906975 | 6.2E-03 | 2.5E-06 |
| 2888 | 75 | 4.73923130002 | 6.0E-03 | 2.3E-06 |
| 3042 | 77 | 4.73897584158 | 5.9E-03 | 2.1E-06 |
| 3200 | 79 | 4.73873186140 | 5.7E-03 | 2.0E-06 |
| 3362 | 81 | 4.73849859998 | 5.6E-03 | 1.8E-06 |
| 3528 | 83 | 4.73827536345 | 5.5E-03 | 1.7E-06 |
| 3698 | 85 | 4.73806151664 | 5.3E-03 | 1.6E-06 |
| 3872 | 87 | 4.73785647701 | 5.2E-03 | 1.5E-06 |
| 4050 | 89 | 4.73765970929 | 5.1E-03 | 1.4E-06 |
| 4232 | 91 | 4.73747072083 | 5.0E-03 | 1.3E-06 |
| 4418 | 93 | 4.73728905739 | 4.9E-03 | 1.2E-06 |
| 4608 | 95 | 4.73711429949 | 4.8E-03 | 1.2E-06 |
| 4802 | 97 | 4.73694605916 | 4.7E-03 | 1.1E-06 |
| 5000 | 99 | 4.73678397699 | 4.6E-03 | 1.0E-06 |

TABLE II: Optimized scale factor for Gaussian exponents for Lebedev quadrature grids with octahedral symmetry. ^{a)}

| N_γ | $Order$ | ζ | σ_γ^{rel} | σ_γ |
|------------|---------|---------------|-----------------------|-----------------|
| 6 | 3 | 4.84566077868 | 2.2E-06 | 3.6E-07 |
| 14 | 5 | 4.86458714334 | 9.0E-04 | 6.5E-05 |
| 26 | 7 | 4.85478226219 | 6.6E-03 | 2.5E-04 |
| 38 | 9 | 4.90105812685 | 1.8E-02 | 4.8E-04 |
| 50 | 11 | 4.89250673295 | 3.8E-03 | 7.8E-05 |
| 86 | 15 | 4.89741372580 | 1.3E-03 | 1.5E-05 |
| 110 | 17 | 4.90101060987 | 5.1E-03 | 4.7E-05 |
| 146 | 19 | 4.89825187392 | 1.4E-02 | 9.9E-05 |
| 170 | 21 | 4.90685517725 | 1.2E-03 | 7.1E-06 |
| 194 | 23 | 4.90337644248 | 3.6E-03 | 1.9E-05 |
| 302 | 29 | 4.90498088169 | 3.2E-03 | 1.1E-05 |
| 350 | 31 | 4.86879474832 | 3.3E-02 | 9.4E-05 |
| 434 | 35 | 4.90567349080 | 2.3E-03 | 5.3E-06 |
| 590 | 41 | 4.90624071359 | 2.0E-03 | 3.4E-06 |
| 770 | 47 | 4.90656435779 | 1.5E-03 | 2.0E-06 |
| 974 | 53 | 4.90685167998 | 1.3E-03 | 1.4E-06 |
| 1202 | 59 | 4.90704098216 | 1.0E-03 | 8.7E-07 |
| 1454 | 65 | 4.90721023869 | 9.6E-04 | 6.7E-07 |
| 1730 | 71 | 4.90733270691 | 7.6E-04 | 4.5E-07 |
| 2030 | 77 | 4.90744499142 | 7.2E-04 | 3.6E-07 |
| 2354 | 83 | 4.90753082825 | 5.8E-04 | 2.5E-07 |
| 2702 | 89 | 4.90760972766 | 5.6E-04 | 2.1E-07 |
| 3074 | 95 | 4.90767282394 | 4.6E-04 | 1.5E-07 |
| 3470 | 101 | 4.90773141371 | 4.4E-04 | 1.3E-07 |
| 3890 | 107 | 4.90777965981 | 3.7E-04 | 9.7E-08 |
| 4334 | 113 | 4.90782469526 | 3.6E-04 | 8.5E-08 |
| 4802 | 119 | 4.90749125553 | 5.0E-04 | 1.1E-07 |
| 5294 | 125 | 4.90762073452 | 4.2E-04 | 8.0E-08 |
| 5810 | 131 | 4.90792902522 | 2.6E-04 | 4.6E-08 |

^{a)}Grids of order 13, 25 and 27 ($N_\gamma=74$, 230 and 266 points, respectively) were neglected due to negative quadrature weights that are not appropriate for use in Eq. 7

FIGURE I: Optimized scale factors for the surface element Gaussian exponents derived from the Gauss-Legendre and Lebedev quadrature formulas. Black diamonds are the optimal zeta values calculated for the Gauss-Legendre surface elements. Black circles and \times symbols are the optimal zeta values calculated for the Lebedev grids of order L given by $L = 6m + 5, \{m = 0, 1, \dots, 21\}$ and $L = 2m + 1, \{m = 1, 2, \dots, 15\}$, respectively. The latter did not fit to the empirical relation of Eq. 12 used to produce the trend-lines. Values for the parameters in Eq. 12 for the Gauss-Legendre surface elements are: $n = 3$, $c_0 = 4.7238274$, $c_1 = 0.21921730$, and $c_2 = 5.6429186$. Corresponding values for the Lebedev surface elements are: $n = 1$, $c_0 = 4.9078341$, $c_1 = -0.84568867$, and $c_2 = 5.5537854$.

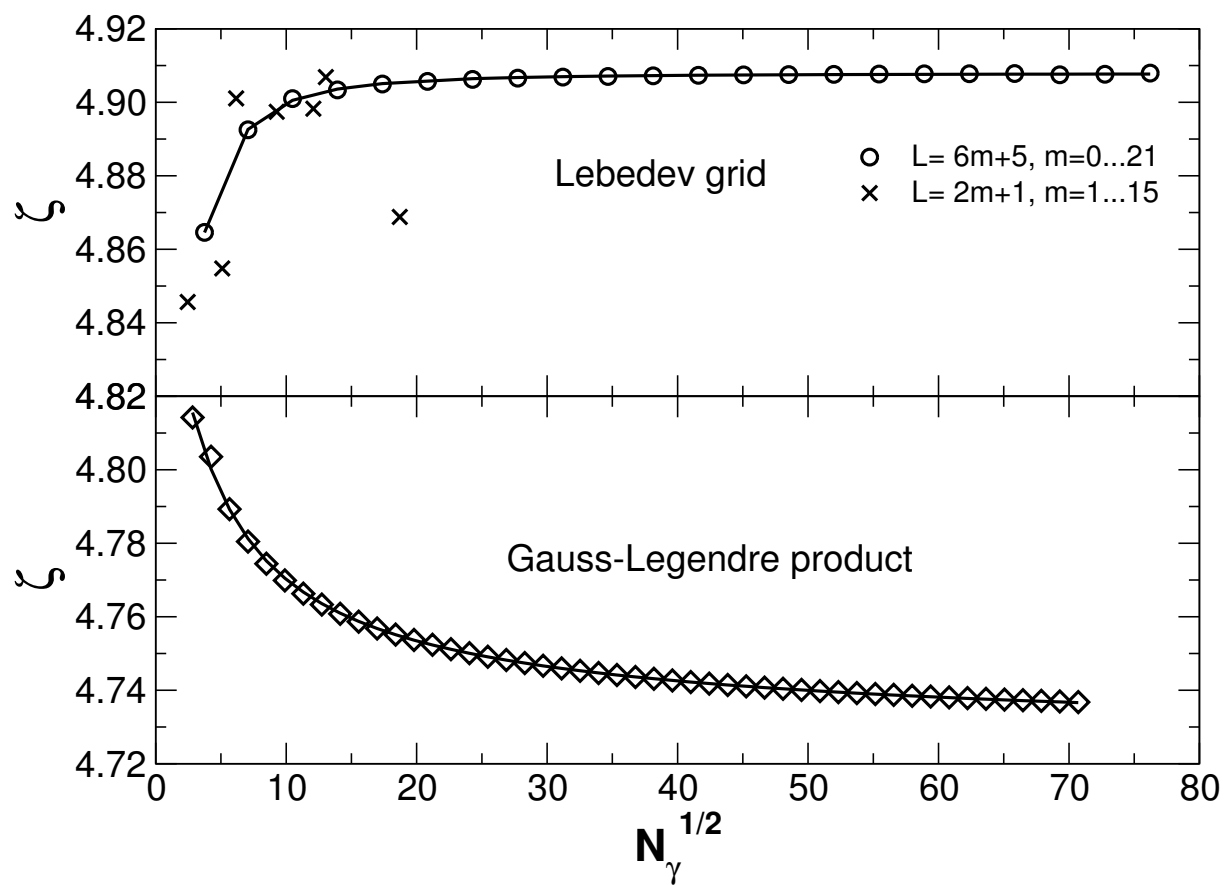


FIGURE I:
B. A. Gregersen and Darrin M. York.